TITLE:

Crystallization Behavior and Structural Stability of Zr50Cu40Al10 Bulk Metallic Glass

AUTHOR(S):

Zhang, Shuo; Ichitsubo, Tetsu; Yokoyama, Yoshihiko; Yamamoto, Tokujiro; Matsubara, Eiichiro; Inoue, Akihisa

CITATION:

Zhang, Shuo ...[et al]. Crystallization Behavior and Structural Stability of Zr50Cu40Al10 Bulk Metallic Glass. MATERIALS TRANSACTIONS 2009, 50(6): 1340-1345

ISSUE DATE:

2009-06

URL:

http://hdl.handle.net/2433/109946

RIGHT:

Copyright (c) 2009 The Japan Institute of Metals

京都大学学術情報リポジトリ
KURENAI 紅
Kyoto University Research Information Repository

京都大学 KYOTO UNIVERSITY
A Self-archived copy in
Kyoto University Research Information Repository
https://repository.kulib.kyoto-u.ac.jp
京都大学学術情報リポジトリ KURENAI 紅 Kyoto University Research Information Repository

Materials Transactions, Vol. 50, No. 6 (2009) pp. 1340 to 1345
©2009 The Japan Institute of Metals

Crystallization Behavior and Structural Stability of $Zr_{50}Cu_{40}Al_{10}$ Bulk Metallic Glass

Shuo Zhang[1,*1], Tetsu Ichitsubo[1,*2], Yoshihiko Yokoyama[2], Tokujiro Yamamoto[2], Eiichiro Matsubara[1] and Akihisa Inoue[2]

[1]*Department of Materials Science and Engineering, Kyoto University, Kyoto 606-8507, Japan*
[2]*Institute for Materials Research, Tohoku University, Sendai 980-8577, Japan*

We have investigated the origin of significantly high thermal stability of $Zr_{50}Cu_{40}Al_{10}$ metallic glass and its crystallization behavior as compared to $Zr_{70}Cu_{20}Al_{10}$ and $Zr_{70}Cu_{30}$ glassy alloys, by differential scanning calorimetry (DSC), x-ray diffraction (XRD) and resonant ultrasound spectroscopy (RUS) techniques. It was found from XRD and DSC analyses that (i) constituent atoms in $Zr_{50}Cu_{40}Al_{10}$ are highly close-packed in a glassy state and (ii) $Zr_{50}Cu_{40}Al_{10}$ glass shows a complicated crystallization process when it is heated at conventional heating rates, but when it is rapidly heated, the ordered B2-type ZrCu is dominantly formed. The high thermal stability and its crystallization behavior are discussed in terms of the long-range-diffusion of atoms and elastic strain energy. [doi:10.2320/matertrans.MBW200833]

(Received October 27, 2008; Accepted March 2, 2009; Published April 22, 2009)

Keywords: *bulk metallic glasses, zirconium-based BMGs, crystallization, rapid heating, structure, differential scanning calorimetry (DSC), field-emission scanning electron microscopy (FE-SEM), X-ray diffraction method, long-range-diffusion, strain energy*

1. Introduction

Bulk metallic glasses, so-called "BMG"s, exhibiting a wide supercooled liquid region have attracted considerable attention not only from engineering aspects but also from glass science perspectives.[1)] They are thermally stable against crystallization, despite the fact that they are mainly composed of relatively-weak metallic bonds and distinct from major glasses having network structures consisting of covalently-bonded clusters or molecules. Inoue's "three experimental rules"[2)] are very helpful to predict and produce stable metallic glasses with high glass-forming ability (GFA), but there are still unsolved problems on the thermal stability, and many researchers have tried to elucidate the origin of the excellent thermal stability of BMGs.

In our opinion, the most important thing in the practical viewpoints is to understand how BMGs can be prevented from crystallization upon heating or thermal process, that is, how the thermal stability of BMGs is enhanced. Here we are now considering four effects for enhancement of the thermal stability of BMGs: (i) closely packing of constituent atoms,[3)] (ii) structural dissimilarity between the amorphous phase and crystallized phase(s),[4)] (iii) necessity of the long-range-diffusion of atoms during crystallization, and (iv) a large amount of the elastic strain energy yielded by crystallization in a glassy solid. In the $Zr_{70}Cu_{30}$ amorphous alloy, for example, the distance of Cu-Cu pairs in amorphous alloy is distinctly different from that in the stable crystalline phase Zr_2Cu.[3,4)] Referring to the structural-dissimilarity aspect, the significant difference in Cu-Cu distance would prevent the crystallization and lead to a stable glass transition. By contrast, crystallization easily occurs in the $Zi_{70}Ni_{30}$ amorphous alloy because of the structural similarity. In addition, the thermal stability of Zr-Cu-Al alloys is markedly varied by the addition of Al element.[3,5–11)] As discussed later, this is mainly because the atomic diffusion of Al atoms is required to form thermally stable crystalline phases. Moreover, the strain-energy concept is a new one for obtaining a stable glass-to-liquid transition, which will be deeply discussed in this paper.

In general, the glass transition temperature (T_g) increases only slightly with increase in a heating rate, whereas the crystallization temperature (T_x) increases significantly. Thus, even in the case that the glass transition is unobservable at usual heating rates (e.g. below 40 K/min), it comes to observable by rapid heating.[12,13)] As mentioned above, since raising the heating rates can significantly affect the crystallization behavior, it is a useful method to investigate the crystallization mechanism or primary crystallization. In this paper, we systematically investigate crystallization process and thermal stability of $Zr_{50}Cu_{40}Al_{10}$ BMG, exhibiting a broad supercooled liquid region, by using differential scanning calorimetry (DSC), X-ray diffraction, field-emission scanning electron microscopy (FE-SEM, JSM-6500F: JEOL). Finally, by estimating the elastic strain energy on the assumption that the crystallization occurs in an amorphous solid, we shall discuss the stable glass-to-liquid transition of the frozen metallic glasses.

2. Experimental

Alloy ingots of $Zr_{50}Cu_{40}Al_{10}$, $Zr_{70}Cu_{30}$, and $Zr_{70}Cu_{20}Al_{10}$ alloys were prepared by arc-melting a mixture of pure Zr, Cu, and Al metals in an argon atmosphere. In order to maintain a low-oxygen concentration in these alloys (especially for $Zr_{50}Cu_{40}Al_{10}$ bulk glass), Zr-crystal rods, specially prepared with oxygen concentration less than 0.05 at%, were used. $Zr_{50}Cu_{40}Al_{10}$ BMG was cast into block-shaped samples of 3 mm × 3 mm × length in dimensions. Ribbon-shaped $Zr_{70}Cu_{20}Al_{10}$ and $Zr_{70}Cu_{30}$ amorphous alloys were prepared by quenching from 1200°C, using a single roller melt-spinning technique in an argon atmosphere with a roller spinning rate at 4000 rpm. The densities of the samples

*1Graduate Student, Kyoto University
*2Corresponding author, E-mail: tichi@mtl.kyoto-u.ac.jp

京都大学 KYOTO UNIVERSITY
A Self-archived copy in
Kyoto University Research Information Repository
https://repository.kulib.kyoto-u.ac.jp
京都大学学術情報リポジトリ KURENAI 紅 Kyoto University Research Information Repository

measured by the Archimedean method are 6.837 g/cm^3 for $Zr_{50}Cu_{40}Al_{10}$, 6.50 g/cm^3 for $Zr_{70}Cu_{20}Al_{10}$ and 7.0 g/cm^3 for $Zr_{70}Cu_{30}$, respectively. The density of the fully crystallized $Zr_{50}Cu_{40}Al_{10}$ is 6.879 g/cm^3.

Differential scanning calorimetry (DSC) measurements were carried out using a standard commercial instrument (Perkin Elmer Diamond DSC) with about 5–10 mg samples. The characteristic temperatures, T_g, T_x, was measured during heating at a constant rate up to $\beta = 500$ K/min, which is the highest β attained in our present instrument. Crystalline phases in the samples after crystallizing in the DSC apparatus were also investigated by X-ray diffraction with CuKα radiation. Structure observation, chemical composition analyses after crystallization were carried out by FE-SEM equipped with an energy dispersion X-ray (EDX) spectrometer.

3. Strain-energy Calculation

In order to evaluate the elastic strain energy supposing that the nucleation of the crystalline phase occurs in "an amorphous solid", we employ the Eshelby inclusion theory.[14,15] In that theory, it is assumed that an ellipsoidal crystalline particle is formed in the original solid glassy matrix, and the strain energy caused by the volume (density) change with crystallization was evaluated by using the following equation:

$$E_{str} = -\frac{1}{2} C_{ijkl}(S_{klmn}\varepsilon^*_{mn} - \varepsilon^*_{kl})\varepsilon^*_{ij}\Omega, \qquad \varepsilon^* = \frac{\sqrt[3]{1/\rho_{Cryst}} - \sqrt[3]{1/\rho_{Amo}}}{\sqrt[3]{1/\rho_{Amo}}} \tag{1}$$

where C_{ijkl}, S_{klmn}, Ω, ε^*_{mn} are the elastic constants, the Eshelby tensor,[14–19] the volume of the inclusion, eigenstrain due to the volume mismatch (i.e., $\varepsilon^*_{mn} = \varepsilon^*\delta_{mn}$ with δ_{mn} the Kronecker delta), respectively, and ρ is the mass density. In the present calculation, we assume that the elastic constants of the crystalline phases are the same as those of the amorphous phase, and we use the elastic constants of the $Zr_{50}Cu_{40}Al_{10}$ BMG measured with the resonant ultrasound spectroscopy (RUS) technique at room temperature.

4. Results and Discussion

4.1 Thermal stability of $Zr_{50}Cu_{40}Al_{10}$ BMG

The characteristic temperatures T_g and T_x of the $Zr_{50}Cu_{40}Al_{10}$ BMG, $Zr_{70}Cu_{20}Al_{10}$, and $Zr_{70}Cu_{30}$ amorphous alloys were measured with DSC from 5 K/min up to 500 K/min. Typical DSC profiles obtained for the $Zr_{50}Cu_{40}Al_{10}$ BMG at various heating rates are shown in Fig. 1(a). The glass transition temperature T_g is defined as the onset temperature of the endothermic reaction, and the crystallization temperature T_x is defined as the onset value of the exothermic peak. Figure 1(b) compared thermal stability of the three Zr-Cu-Al alloys; the T_g and T_x values for the three alloys are plotted against log β. It is found that these characteristic temperatures can be expressed in Lasocka's empirical form.[20]

$$T_{x,g} = a_{x,g} + b_{x,g} \log \beta \tag{2}$$

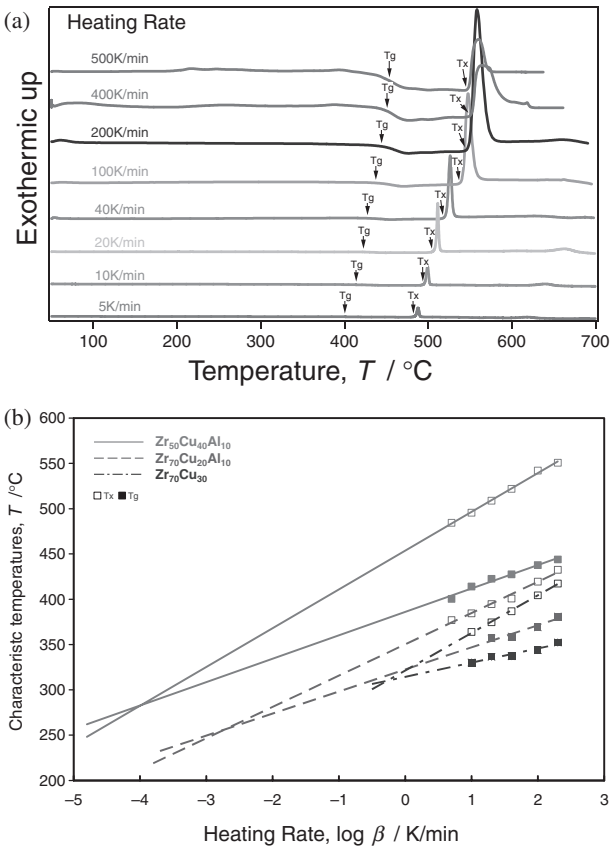

Fig. 1 (a) DSC profiles at various heating rates for $Zr_{50}Cu_{40}Al_{10}$. (b) Heating-rate dependence of T_g and T_x of $Zr_{50}Cu_{40}Al_{10}$, $Zr_{70}Cu_{20}Al_{10}$, and $Zr_{70}Cu_{30}$.

Table 1 The β_c values for respective metallic glasses.

Glasses	β_c (K/min)
$Zr_{50}Cu_{40}Al_{10}$	1.0×10^{-4}
$Pd_{42.5}Ni_{7.5}Cu_{30}P_{20}$	7.2×10^{-4}
$Zr_{70}Cu_{20}Al_{10}$	2.0×10^{-2}
$Zr_{65}Al_{7.5}Ni_{10}Pd_{17.5}$	5.5×10^{-3}
$Zr_{65}Al_{7.5}Ni_{10}Cu_{17.5}$	5.9×10^{-3}
$Zr_{70}Cu_{30}$	1.0×10^{0}
$Zr_{70}Ni_{30}$	1.7×10^{1}

Ichitsubo *et al.* reported that the intersection point of the two fitted lines of T_g and T_x in the Lasocka plot, β_c, is one of indices for evaluating the thermal stability of BMGs. In general, the maximum diameter is frequently used for evaluation of GFA, which is an index of stability during a cooling process. In contrast, the parameter β_c used here is an index for the thermal stability of the glassy solid during a heating process. A more stable BMG tends to exhibit a smaller value of β_c. Table 1 summarizes the β_c values of several BMGs obtained from the present experiment and our previous experiments.[4,13] The value of β_c of the $Zr_{50}Cu_{40}Al_{10}$ BMG is found to be quite small and comparable to that of the $Pd_{42.5}Ni_{7.5}Cu_{30}P_{20}$ BMG which is well known as the highest glass former among metallic glasses. This indicates that $Zr_{50}Cu_{40}Al_{10}$ can also be regarded as one of the most stable BMGs. It is interesting to note that β_c of the $Zr_{70}Cu_{20}Al_{10}$ glass is significantly

京都大学 KYOTO UNIVERSITY
A Self-archived copy in
Kyoto University Research Information Repository
https://repository.kulib.kyoto-u.ac.jp
京都大学学術情報リポジトリ KURENAI 紅 Kyoto University Research Information Repository

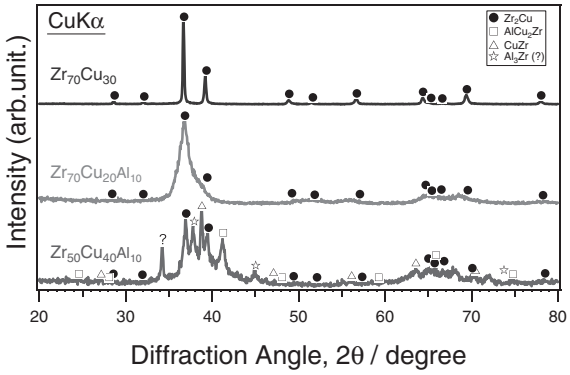

Fig. 2 XRD profiles obtained for the samples heated just above the crystallization temperature of respective glasses.

smaller than that of the binary $Zr_{70}Cu_{30}$ amorphous alloy, despite the fact that ΔT_x ($\equiv T_x - T_g$) of the two glasses are not largely different. Thus, it is found that the three glasses show significant differences in terms of the thermal stability, although they are composed of the same constituent elements.

According to the structural analyses by X-ray diffraction for $Zr_{70}Cu_{20}Al_{10}$ and $Zr_{70}Cu_{30}$ amorphous alloys,[3] the total coordination numbers around each constituent element are approximately 10. In contract, the extremely high total coordination numbers exceeding 11 around all constituent elements in $Zr_{50}Cu_{40}Al_{10}$ are only realized in a homogeneously close-packed glassy structure. Additionally, average number densities of atoms (ρ_0) were calculated by

$$\rho_0 = \frac{N_A}{\bar{M}}\rho_S, \quad \bar{M} = M_{Zr}X_{Zr} + M_{Cu}X_{Cu} + M_{Al}X_{Al}, \quad (3)$$

where N_A, ρ_S, and $\bar{M}$ are the Avogadro number, sample mass density, and the average molecular mass, which is calculated using the atomic mass numbers of each constituent element ($M_{Zr} = 91.22$, $M_{Cu} = 63.55$, $M_{Al} = 26.98$) and the compositions (X_{Zr}, X_{Cu}, X_{Al}). The ρ_0 values of respective glasses are $Zr_{50}Cu_{40}Al_{10}$: 0.0537 (1/Å^3), $Zr_{70}Cu_{20}Al_{10}$: 0.0494 (1/Å^3), $Zr_{70}Cu_{30}$: 0.0508 (1/Å^3). The relatively high ρ_0 value of $Zr_{50}Cu_{40}Al_{10}$ BMG is also an indication of the homogeneously close-packed glassy structure.

Next, we discuss the crystallization behaviors of the respective glasses. Figure 2 shows the X-ray diffraction profiles of the samples after heated just above the crystallization temperature. Each sample was heated in the DSC furnace at $\beta = 40$ K/min, the DSC measurement was terminated at the temperature where the exothermic reaction ended ($Zr_{50}Cu_{40}Al_{10}$: 522°C, $Zr_{70}Cu_{20}Al_{10}$: 398°C, $Zr_{70}Cu_{30}$: 389°C), and subsequently the sample was cooled down quickly to ambient temperature. After that, we have investigated the crystalline phases in the samples by X-ray diffraction. As is found from Fig. 2, the crystallization process is rather simple in both cases of $Zr_{70}Cu_{20}Al_{10}$ and $Zr_{70}Cu_{30}$ and the main crystalline phase is Zr_2Cu with $C11_b$ structure. By contrast, $Zr_{50}Cu_{40}Al_{10}$ shows a complicated crystallization process, and the resulted crystalline phases are plural; apart from the principal Zr_2Cu crystalline phase, $AlCu_2Zr$ (one of equilibrium phases in $Zr_{50}Cu_{40}Al_{10}$) and B2-type ZrCu (equilibrium phase higher than 715°C[21,22]) are

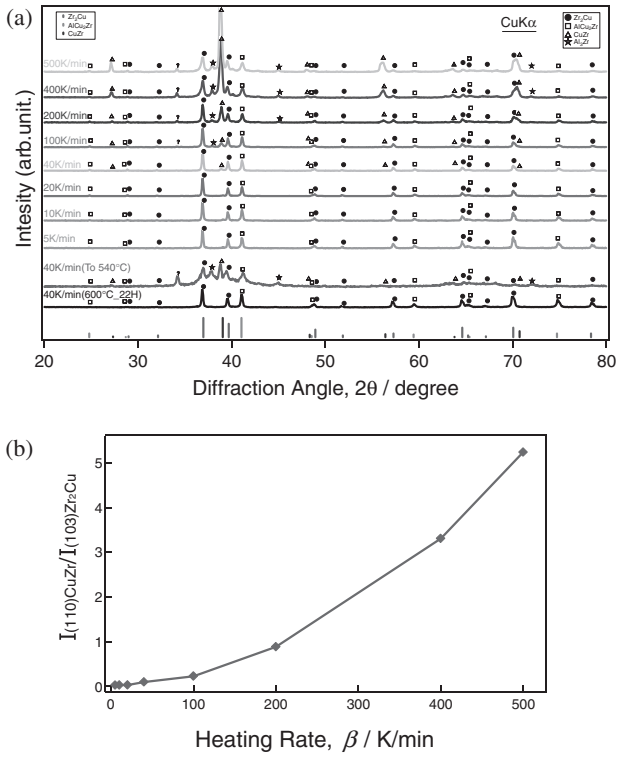

Fig. 3 (a) XRD profiles obtained for the $Zr_{50}Cu_{40}Al_{10}$ glass heated to 700°C at respective heating rates. (b) The intensity ratio of two diffraction peaks (110 from B2 CuZr and 103 from $C11_b$ Zr_2Cu) after crystallized at various rates.

also formed. Especially, the latter phase, B2-type ZrCu, is a non-equilibrium phase, and this singular formation is deeply discussed in the later section. For such as a complicated crystallization process including phase separation, long-range diffusion of atoms is generally required. Thus, it is considered that long-range diffusion of atoms plays an important role of retarding/preventing the crystallization in the $Zr_{50}Cu_{40}Al_{10}$ BMG.

4.2 Formation of B2-type ZrCu phase in $Zr_{50}Cu_{40}Al_{10}$ BMG

In order to clarify the complicated crystallization of the $Zr_{50}Cu_{40}Al_{10}$ BMG, we focus on the heating-rate dependence of its crystallization behavior. As is seen in Fig. 1(a), the supercooled liquid region (ΔT_x) of $Zr_{50}Cu_{40}Al_{10}$ is as broad as 100 K, even when β is less than 40 K/min. It is seen that ΔT_x becomes broader at a higher β, because the increase in T_x with increasing β is much steeper than that in T_g. Since the crystallization of the amorphous phase generally requires atomic diffusion, when β is higher it is more difficult to gain sufficient atomic diffusion distance for crystallization.

Figure 3(a) shows XRD profiles obtained for the $Zr_{50}Cu_{40}Al_{10}$ BMG heated up to 700°C at respective heating rates. The profiles of the sample heated up to the end of exothermic peak of crystallization (540°C) and of the fully crystallized sample (annealed for 2 h after heated up to 600°C) were also displayed for reference. Despite the fact that the main crystalline phases of $Zr_{50}Cu_{40}Al_{10}$ are usually tetragonal Zr_2Cu and cubic $AlCu_2Zr$, the ordered B2-type ZrCu is formed more markedly when the heating rate

京都大学 KYOTO UNIVERSITY
A Self-archived copy in
Kyoto University Research Information Repository
https://repository.kulib.kyoto-u.ac.jp
京都大学学術情報リポジトリ KURENAI 紅 Kyoto University Research Information Repository

Table 2 Interatomic distances and coordination number in $Zr_{50}Cu_{40}Al_{10}$ and B2-ZrCu.

	$Zr_{50}Cu_{40}Al_{10}$		ZrCu	
	r [nm]	N	r [nm]	N
Zr-Zr	0.323	5.8	0.322	6
Zr-Cu	0.286	4.7	0.279	8
Zr-Al	0.305	1.3	—	—
Total		11.8		14
Cu-Zr	0.286	5.9	0.279	8
Cu-Cu	0.265	4.0	0.322	6
Cu-Al	0.269	0.9	—	—
Total		10.7		14

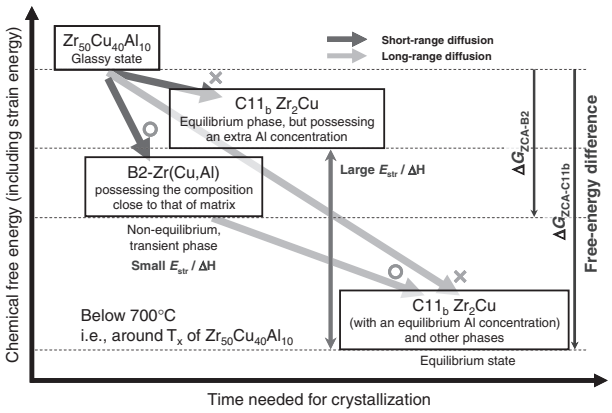

Fig. 4 Schematic diagram showing the decrease of the chemical-free-energy accompanied by the crystallization process. The solid (red) arrows indicate the crystallization process driven by the short-range diffusion, and the hatched (blue) arrows indicate the long-range-diffusion process.

becomes higher. This is summarized in Fig. 3(b), which shows the intensity ratio of two X-ray diffraction peaks (110 from ZrCu and 103 from Zr_2Cu) after crystallized at various rates. As far as we know, this is the first time to report that B2-type ZrCu is formed in the Zr-Cu-Al metallic glass system.

In the case of a higher β, the spent time till reaching a certain temperature is shortened, which means that a higher β reduces the annealing time at sufficiently high temperatures where atomic diffusion appreciably takes place, that is, the long-range diffusion of atoms enough for crystallization cannot be taken place. In other words, the present result strongly means that, when a glass phase has to be crystallized without long-range diffusion of atoms, it tends to transform into a crystalline phase as the primary phase, that possesses a similar composition and/or structure to those of the parent glass phase.

Table 2 compares the local structure of the $Zr_{50}Cu_{40}Al_{10}$ BMG determined by X-ray diffraction[3] and the structure of B2-type ZrCu.[21,22] The Zr-Cu distance in $Zr_{50}Cu_{40}Al_{10}$ is 0.286 nm, being very close to the distance (0.279 nm) of the nearest neighbor Zr-Cu pair in B2 ZrCu. In addition, the Zr-Zr distance (0.323 nm) in $Zr_{50}Cu_{40}Al_{10}$ is also close to the distance (0.323 nm) of the next nearest neighbor Zr-Zr pair in B2-type ZrCu. Thus, it may be possible to say that the local structures of the original glassy matrix and the ordered B2-type ZrCu have certain similarities in terms of the interatomic distances and atomic coordination. Here, we encounter a new problem, that is, we have to consider why the B2 phase is not easily formed in the usual crystallization behavior of the $Zr_{50}Cu_{40}Al_{10}$ BMG.

As is mentioned above, the ordered B2-type ZrCu is a high-temperature equilibrium phase (higher than 715°C[21,22] in the binary alloy); hence, around about 650°C (this was the maximum temperature in the present DSC experiments), the B2-type ZrCu phase is a non-equilibrium phase. Thus, as is seen in Fig. 4, it is naturally expected that the driving force for the transformation into the ordered B2-type ZrCu phase should be not so large, compared to that for the transformation into the thermodynamically equilibrium phases such as $C11_b$-type Zr_2Cu and the others. Repeatedly to say, long-range diffusion is required for the latter crystallization process including the phase separation. Consequently, $Zr_{50}Cu_{40}Al_{10}$ possesses a considerable high thermal stability among metallic glasses.

4.3 Effect of elastic strain energy

It is well known that the elastic strain contributes to retarding or prohibiting the nucleation in a mother phase. Therefore, for discussing the presence or absence of stable glass-to-liquid transition of metallic glasses, it is meaningful to evaluate the elastic strain energy associated with the crystallization. For the purpose of the present calculation, we consider that the nucleation of the crystalline phase occurs in the solid amorphous matrix.

Table 3 summarizes the results of the calculated elastic strain energy, E_{str}, caused by crystallization in several glasses. The elastic strain energy was calculated using the expected mass density, ρ_{Cryst}, of the crystal, which is estimated under the condition that the single phase with the B2 or $C11_b$ structure of the lattice parameters measured by X-ray diffraction contains the constituent atoms in accordance with the atomic compositions of the mother glass. The crystallization heat, ΔH, was obtained from the DSC profile at $\beta = 40$ K/min. The elastic constants reported by Zhang *et al.*[3] were used in the present calculation.

Since the crystallization heat is the enthalpy difference between the amorphous state and crystallized state, we may regard that the driving force of crystallization is approximately proportional to the magnitude of ΔH. On the other hand, the strain energy caused by the volume (density) change accompanied by the crystallization should be a positive effect on preventing the crystallization. Therefore, it is reasonable to claim that the stable glass-to-liquid transition will appear when the magnitude of $E_{str}/\Delta H$ cannot be neglected, because the nucleation of crystals becomes easier in the supercooled liquid state that has softer elastic constants. As is seen in Table 3, the $E_{str}/\Delta H$ value for the $Zr_{70}Cu_{30}$ amorphous alloy is considerably smaller than the values of $Zr_{50}Cu_{40}Al_{10}$ and $Zr_{70}Cu_{20}Al_{10}$ metallic glasses. Thus, a large amount of the elastic strain energy, i.e., large value of $E_{str}/\Delta H$, contributes to the prevention of crystallization, which leads to the excellent thermal stability of BMGs.

Here we especially focused on the strain energy associated with the volume change by crystallizing to sound out

京都大学 KYOTO UNIVERSITY
A Self-archived copy in
Kyoto University Research Information Repository
https://repository.kulib.kyoto-u.ac.jp
京都大学学術情報リポジトリ KURENAI 紅 Kyoto University Research Information Repository

Table 3 The elastic strain energy caused by crystallization.

	$Zr_{50}Cu_{40}Al_{10}$		$Zr_{70}Cu_{20}Al_{10}$	$Zr_{70}Cu_{30}$
Density of glass phase, ρ_{Amo} (10^3 kg/m^3)	6.90		6.5	7.0
Crystallization heat by DSC, ΔH (J/g)	46.5		52.7	83.7
Crystalline phase supposed to be formed	B2 ZrCu	$C11_b$ Zr_2Cu	$C11_b$ Zr_2Cu	$C11_b$ Zr_2Cu
Measured lattice parameters by X-ray (Å)	$a = 3.28$	$a = 3.22$ $c = 11.2$	$a = 3.22$ $c = 11.2$	$a = 3.24$ $c = 11.3$
*Expected mass density of crystal, ρ_{Cryst} (10^3 kg/m^3)	6.94	6.33	6.81	7.01
Measured strain energy, E_{str} (J/g)	0.40	15.3	5.16	0.003
$E_{str}/\Delta H$	0.9%	32.8%	9.8%	0.004%

*The expected mass density, ρ_{Cryst}, of the crystal is estimated under the condition that the single phase with the B2 or $C11_b$ structure of the lattice parameters measured by X-ray contains the constituent atoms in accordance with the atomic compositions of the mother glass.

any other origin of the formation of B2 ZrCu as the primary phase instead of an equilibrium $C11_b$ Zr_2Cu phase. From the FESEM-EDX analysis, we have found that the compositional deviation of Al from the composition of the mother glass is less than 2 at% even after annealing at a sufficiently high temperature for long duration (600C, 22 h). Thus, it appears to be reasonable to assume that the $C11_b$-type Zr_2Cu crystalline phase is formed with the same composition of the $Zr_{50}Cu_{40}Al_{10}$ mother glass. Since the composition of Zr_2Cu is obviously different from the original glass, a large quantity of Cu and Al atoms have to occupy the Zr sites in Zr_2Cu instead of Zr atoms on the present assumption. Thus, the density of $C11_b$-type Zr_2Cu is expected to decrease, being far from the mass density of the glass matrix, so that the value of $E_{str}/\Delta H$ inevitably amounts to about 30%, if such a crystalline phase is supposed to be formed in the glass matrix. Thus, we can understand from the viewpoints of the strain energy that the formation of the equilibrium Zr_2Cu phase in the glassy solid is quite unlikely. Therefore, in order for the $Zr_{50}Cu_{40}Al_{10}$ glass to be crystallized easily, first the glass matrix has to become softer by transforming into a supercooled liquid, and then long-range diffusion of Cu and Al atoms are required for the complicated crystallization process including a phase separation.

On the other hand, although B2-type ZrCu is a high-temperature equilibrium phase, the strain energy is not so large for the crystallization to B2-type ZrCu, and furthermore long-range diffusion of Al atoms is not required because the composition is similar to that of the original glass matrix, resulting in the facile crystallization toward B2-type ZrCu.

5. Conclusion

We have investigated the complicated crystallization behavior and origin of the high thermal stability of the $Zr_{50}Cu_{40}Al_{10}$ BMG, by comparing to $Zr_{70}Cu_{30}$ and $Zr_{70}Cu_{20}Al_{10}$ amorphous alloys. The salient results are summarized as follows:

(1) The $Zr_{50}Cu_{40}Al_{10}$ BMG has a homogeneously close-packed glassy structure, compared to the other amorphous alloys.
(2) It is found that the unusual B2-type ZrCu crystalline phase is mainly formed when the glass is rapidly heated up. The reason of formation of the B2 phase is that the long-range diffusion cannot take place sufficiently in the case of high heating rates and, hence, the B2-type ZrCu phase possessing a similar composition to that of the glass matrix is favored to be formed. From this result, it is considered that the B2 phase is probably a primary phase in the usual crystallization.
(3) The B2-type ZrCu is a high-temperature phase and not an equilibrium phase around T_g and T_x of the glass; therefore, the driving force of the crystallization toward the B2 phase is considered to be lower than that in the case of the crystallization to the equilibrium phases (e.g., Zr_2Cu), and furthermore long-range diffusion is inevitable required for the latter crystallization process including the phase separation. This is an origin of the high thermal stability and main reason for retarding the crystallization in the $Zr_{50}Cu_{40}Al_{10}$ BMG.
(4) It is considered that the elastic strain plays a key role in the presence of the stable glass-to-liquid transition of Zr-M and Zr-Al-M (M=Cu, Ni) metallic glasses. It is found that the ratio of the strain energy to the crystallization heat ($E_{str}/\Delta H$) of the $Zr_{50}Cu_{40}Al_{10}$ BMG is the highest between the three glasses. Moreover, the value of $E_{str}/\Delta H$ of $Zr_{70}Cu_{20}Al_{10}$ exceeds that of $Zr_{70}Cu_{30}$. This indicates that the value of $E_{str}/\Delta H$ reflects the thermal stability of the metallic glasses upon heating treatments.

Acknowledgements

This work was partly supported by Grant-in-Aid for Scientific Research on the Priority Area Investigation of “Materials Science of Bulk Metallic Glasses” from the Ministry of Education, Culture, Sports, Science and Technology, Japan.

京都大学 KYOTO UNIVERSITY
A Self-archived copy in
Kyoto University Research Information Repository
https://repository.kulib.kyoto-u.ac.jp
京都大学学術情報リポジトリ KURENAI 紅 Kyoto University Research Information Repository

REFERENCES

1) A. Inoue: Acta Mater. **48** (2000) 279.
2) A. Inoue, T. Zhang and T. Masumoto: Mater. Trans. JIM **30** (1989) 965–972.
3) S. Zhang, T. Ichitsubo, Y. Yokoyama, K. Miyagi and E. Matsubara: Mater. Sci. Forum **561–565** (2007) 1391.
4) T. Ichitsubo, E. Matsubara, J. Saida and H. S. Chen: Mater. Trans. **46** (2005) 2282–2286.
5) Y. Yokoyama, K. Inoue and K. Fukaura: Mater. Trans. **43** (2002) 3199–3205.
6) K. Nakayama, Y. Yokoyama, G. Xie, Q. S. Zhang, M. W. Chen, T. Sakurai and A. Inoue: Nano Lett. **8** (2008) 516.
7) Y. Yokoyama, T. Yamasaki, P. K. Liaw, R. A. Buchanan and A. Inoue: J. Alloy. Compd. **434–435** (2007) 160.
8) Y. Yokoyama, Y. Akeno, T. Yamasaki, P. K. Liaw, R. A. Buchanan and A. Inoue: Mater. Trans. **46** (2005) 2755–2761.
9) T. Yano, Y. Yorikado, Y. Akeno, F. Hori, Y. Yokoyama, A. Iwase, A. Inoue and T. J. Konno: Mater. Trans. **46** (2005) 2886–2892.
10) Y. Yokoyama, H. Inoue, K. Fukaura and A. Inoue: Mater. Trans. **43** (2002) 575–579.
11) Y. Yokoyama, H. Fredriksson, H. Yasuda, M. Nishijima and A. Inoue: Mater. Trans. **48** (2007) 1363–1372.
12) T. Ichitsubo, E. Matsubara, H. Numakura, K. Tanaka, N. Nishiyama and R. Tarumi: Phys. Rev. B **72** (2005) 052201.
13) E. Matsubara, T. Ichitsubo, J. Saida, S. Kohara and H. Ohsumi: J. Alloy. Compd. **434** (2007) 119.
14) J. D. Eshelby: Proc. R. Soc. London Sect. A **241** (1957) 376.
15) T. Mura: *Micromechanics of defects in solids*, 2nd ed., revised., (Martinus Nijhoff, United States, 1987).
16) T. Ichitsubo, D. Koumoto, M. Hirao, K. Tanaka, M. Osawa, T. Yokohawa and H. Harada: Acta Mater. **51** (2003) 4033.
17) T. Ichitsubo, M. Nakamoto, K. Tanaka and M. Koiwa: Mater. Trans. JIM **39** (1998) 24–30.
18) T. Ichitsubo, K. Tanaka, M. Koiwa and Y. Yamazaki: Phys. Rev. B **62** (2000) 5435.
19) K. Hirai, T. Ichitsubo, T. Uda, A. Miyazaki 1, S. Yagi and E. Matsubara: Acta Mater. **56** (2008) 1539.
20) M. Lasocka: Mater. Sci. Eng. **23** (1976) 173.
21) Binary Alloy Phase Diagrams, Second Edition, Ohio (1990) 2.
22) Binary Alloy Phase Diagrams, Second Edition, Ohio (1990) 1511.